Dynamic aspects in host–guest interactions. Part 4. Kinetic and ^{1}H NMR evidence for multi-step directional binding in the molecular recognition of some 2-naphthylazophenol guests with α-cyclodextrin

Noboru Yoshida
Laboratory of Molecular Functional Chemistry, Division of Material Science, Graduate School of Evironmental Earth Science, Hokkaido University, Sapporo 060, Japan

Detailed solution kinetic and equilibria data in aqueous solution are presented for the molecular recognition by α-cyclodextrin (α-CD_x) of structually different types of 2-naphthylazophenol guest. ^{1}H NMR equilibrium titrations and stopped-flow data have allowed the determination of the proposed structure of the intermediate, equilibrium constants, and the rate and mechanism for the molecular recognition by α-cyclodextrin. Some kinetic data are consistent with a two-step inclusion process wherein the intramolecular structural reorganization from the intermediate to the final inclusion complex is the rate-controlling step. ^{1}H NMR data also support the existence of stable intermediate species. The steric and charge factors affecting the directional inclusion process are discussed.

Introduction

The molecular recognition phenomena by cyclodextrins have been a subject of special attention in the past decade as suitable models for enzyme–substrate binding and subsequent catalytic processes.[1] Recently, some progress has been made in understanding the mechanism of the molecular recognition by α-cyclodextrin[2–5] and hexakis(di-*O*-methyl)-α-cyclodextrin.[3f] For example, the inclusion reactions of a series of 1-naphthylazophenol guests (*vide infra*) proceed according to a simple one-step binding mechanism.[2,3b,c]

$$\text{Guest (G)} + \alpha\text{-CD}_x \underset{k_b}{\overset{k_f}{\rightleftharpoons}} \text{G-}\alpha\text{CD}_x \qquad (1)$$

Inclusion of the naphthalenesulfonate moiety (direction B) by α-CD_x is sterically impossible and only inclusion from the alkylphenol side of the guest (direction A) is possible. Therefore, the charge and steric factors concerning the

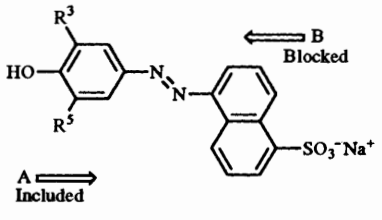

alkylphenol moiety of the guests are particularly important in influencing the kinetics. The equilibrium constants are largely unchanged, but the rate constants (k_f and k_b) are quite sensitive to the alkyl substituent groups (R^3 and R^5) on the phenol ring. Furthermore, a significant decrease in the rate constants k_f and k_b has been observed when the degree of the hydration at the periphery of the hydroxy group changes upon ionization from OH to O^-.[2,3c] These observations support conclusively the inclusion from direction A.

In a recent study on the inclusion reactions of α-cyclodextrin with alkyl-substituted hydroxyphenylazo derivatives of sulfanilic acid, it was demonstrated that the rate, mechanism and direction of inclusion are critically dependent on the size and shape of the alkyl substituents (R^3 and R^5).[3d,e]

Two types of inclusion from direction **A** or **B** are possible

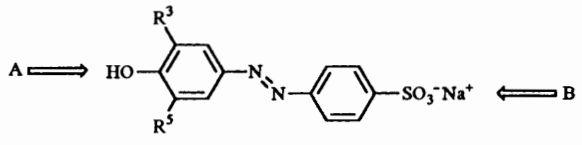

depending upon the position, size and shape of the alkyl substituents. In the guest systems (R^3 = R^5 = Me and Pr^i), inclusion from direction **A** is fully blocked owing to the steric hindrance of dimethyl or di-isopropyl groups. The inclusions of the guests (R^3 = Et, Pr, Pr^i and Bu^t; R^5 = H) with α-CD_x may proceed from direction **B** and *via* a two-step mechanism: (*a*) fast binding of the guest with the host yielding an intermediate species and (*b*) slow intramolecular structural reorganization of the intermediate yielding a final stable inclusion complex. The relative importance of these two steps depends on steric factors such as the size and shape of the alkyl substituents.

On the basis of these earlier observations, we have investigated the relationship between the kinetics and the structural aspects of the inclusion process by α-CD_x of some azo guest molecules **1**–**8**, which contain the 2-naphthyl moiety, in order to elucidate further the mechanism of the inclusion process by α-CD_x.

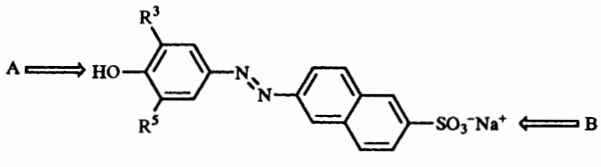

	R^3	R^5		R^3	R^5
1	H	H	**5**	Pr^i	H
2	Me	H	**6**	Bu^t	H
3	Et	H	**7**	Me	Me
4	Pr	H	**8**	Pr^i	Pr^i

Experimental

Materials

The sodium salts of 2-naphthylazo guest molecules were prepared as described previously and purified by liquid-column

Table 1 Formation constants (K_f, K_f'/dm^3 mol^{-1})[a] for the α-CD_x inclusion complexes with the acid form (HA^-) and the base form (A^{2-}) of some 2-naphthylazophenol guest molecules

Guest molecule	pK_a	λ_{max}/nm				K_f/dm^3 mol^{-1}	K_f'/dm^3 mol^{-1}
		HA^-	HA^-–αCD_x	A^{2-}	A^{2-}–αCD_x		
1 (R_3 = H)	7.85	362	372	450	426	6 300	6 200
2 (R_3 = Me)	8.16	365	370	460	445	11 000	9 700
3 (R_3 = Et)	8.36	370	374	465	450	14 000	6 900
4 (R_3 = Pr)	8.46	370	377	465	455	9 800	4 700
7 (R_3,R_5 = Me)	8.21	367	372	475	461	5 000	4 300

[a] At 25 °C and I = 0.1 mol dm^{-3} (NaCl). Error limits are estimated to be not larger than ± 10%.

chromatography.[3c] Their elemental analyses showed excellent agreement with those calculated from the formulae. α-CD_x was purchased from Tokyo Kasei Chemicals Co. and used without further purification. The pH of the solution in the acidic and alkaline regions was maintained with phosphate buffer (pH 4.2–4.5) and NaOH (pH 11.0–11.5), respectively. The ionic strength was maintained at 0.1 mol dm^{-3} with NaCl.

Measurements

VIS and UV spectra were obtained on a JASCO Ubest-30 recording spectrophotometer. A Hitachi–Horiba Model F-7ss pH meter was used for pH measurements. Acid dissocation constants (K_a) and the stability constants (K_f) were determined spectrophotometrically. Reaction rates were followed spectroscopically using a Unisoku optical fibre type stopped-flow apparatus. A water-jacketed optical cell thermostatted to within ± 0.1 °C with fused silica windows and an optical path length of 10 cm was used. Pseudo-first-order conditions of a large excess α-CD_x concentrations were maintained over guest concentrations {[guest] = (2–5) × 10^{-5} mol dm^{-3}}. ^{1}H NMR spectra of the inclusion complexes were taken on a JEOL JNM-GX270 FT NMR spectrometer (270 MHz) in a 5 mm spinning tube at 25 °C (pD = 3.5 for HA^-–αCD_x and pD = 12.2 for A^{2-}–αCD_x). D_2O (99.9%), NaOD and 20% DCl were purchased from Merck. Values of the chemical shift are referred to external tetramethylsilane (1% TMS in $CDCl_3$). For the continuous spectral measurements, 400 μl solutions of guests (typically 5 mg) were titrated with consecutive additions of solid α-CD_x (0.5–21 mg). The resulting solutions were thoroughly mixed and allowed to equilibrate for several minutes in the probe before the spectrum was acquired. The value of bound (%) defined as the % ratio of the complexed guest to the total guest varied between 0 and *ca.* 100%.

Results and discussion

Inclusion stability constants

The azo guests **1–8** exist as the monovalent acid form (HA^-) at pH 4.0–4.2 and the divalent base form (A^{2-}) at pH 11–11.5, where H denotes the phenol proton (–$R^3R^5C_6H_2OH$). Only the 1 : 1 (host : guest) inclusion model fits the optical titration data using the UV–VIS spectral change. The clear existence of isosbestic points and Hildebrand–Benesi plot support the following simple 1 : 1 inclusion equilibria.

$$HA^- + \alpha\text{-}CD_x \overset{K_f}{\rightleftharpoons} HA^-\text{-}\alpha CD_x \quad (2)$$

$$A^{2-} + \alpha\text{-}CD_x \overset{K_f'}{\rightleftharpoons} A^{2-}\text{-}\alpha CD_x \quad (3)$$

The Hildebrand–Benesi equations gave the stability constants of K_f = 5000 dm^3 mol^{-1} and K_f' = 4300 dm^3 mol^{-1} for **7** (HA^-) and **7** (A^{2-}), respectively. The stability constants K_f and K_f' presented in Table 1 are found to be largely unchanged when the alkyl substituents (R^3 and R^5) of **1–4** and **7** are varied, although the inclusion complex of **3** (HA^-) is the most stable. The general tendency of stability constants ($K_f > K_f'$)[3c] is also observed in these guest systems. The inclusion of **6**, **7** and **8** by α-CD_x is fully blocked from direction **A** because the bulky alkylphenol side of these guests are too large to be incorporated into the α-CD_x cavity. Therefore, only inclusion from the direction **B** is possible. Further steric repulsion between the rim of α-CD_x and the bulky alkyl groups such as Bu^t, di-Pr^i and di-Me is observed. In particular, the stability of **6** and **8** decreased considerably as $K_f(HA^-)$ = 1300 dm^3 mol^{-1} and $K_f(HA^-)$ = 1200 dm^3 mol^{-1}, respectively. As regards inclusion from direction **B** (naphthalenesulfonate moiety), the position of the sulfonate group is important. For example, the

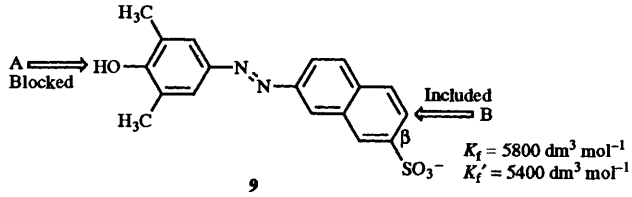

9

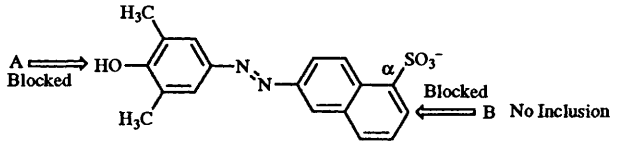

10

β-position of the $-SO_3^-$ group in **9** did not change the stability (K_f = 5800 and K_f' = 5400 dm^3 mol^{-1}) as compared with that in **7**. On the other hand, the α-position of the $-SO_3^-$ group as in **10** inhibits completely the incorporation from the direction **B** owing to a greater degree of steric hindrance.

Rates and mechanism

Generally, single-exponential signals have been observed in most inclusion reactions of α-CD_x with 1-naphthylazo guest molecules.[2–4] The observed rate constant (k_{obsd}) for the following simple 1 : 1 (host : guest) inclusion reaction increases linearly with the concentration of α-CD_x.

$$\text{Guest (G)} + \alpha\text{-}CD_x \underset{k_{-1}}{\overset{k_{+1}}{\rightleftharpoons}} \text{G-}\alpha CD_x \quad (4)$$

$$k_{obsd} = k_{+1}[\alpha\text{-}CD_x]_T + k_{-1} \quad (5)$$

However, in some of our 2-naphthylazo guest systems, two distinct absorbance changes at 500 nm are observed in the fast (1 s) and slow (20 s) time regions. A plot of k_{obsd}(fast) *vs.* [α-CD_x]$_T$ is linear and that of k_{obsd}(slow) is curved and approaches a saturated value in the higher [α-CD_x]$_T$ concentration.

Generally, these concentration dependences of k_{obsd} can be simply interpreted in terms of the following two-step inclusion mechanism,[3d,e,4b,5] where the first step may be a fast association process between the guest and the host and the subsequent step a slower structural reorganization process of the intermediate species G/α-CD_x* which is in slower equilibrium with a more stable inclusion complex G/α-CD_x. If the first step is very fast compared with the second step in eqn. (6), the observed rate constant k_{obsd} could be expressed by eqns. (7) and (8), where

$$\text{Guest (G)} + \alpha\text{-CD}_x \underset{k_{-1}}{\overset{k_{+1}}{\rightleftharpoons}} \text{G/}\alpha\text{-CD}_x^* \underset{k_{-2}}{\overset{k_{+2}}{\rightleftharpoons}} \text{G/}\alpha\text{-CD}_x \quad (6)$$

(fast) (slow)

$$k_{obsd}(\text{fast}) = k_{+1}[\alpha\text{-CD}_x]_T + k_{-1} \quad (7)$$

$$k_{obsd}(\text{slow}) = \frac{K_1 k_{+2}[\alpha\text{-CD}_x]_T}{(1 + K_1[\alpha\text{-CD}_x]_T} + k_{-2} \quad (8)$$

$K_1 = k_{+1}/k_{-1}$. The concentration dependences of k_{obsd} coincide well with the rate expressions shown in eqns. (7) and (8). The calculated rate constants k_{+1}, k_{-1}, k_{+2} and k_{-2} and the equilibrium constant K_1 are summarized in Table 2.

The two-step inclusion mechanism mentioned above was found in such guest systems as **2** (A^{2-}), **3** (HA^- and A^{2-}), **4** (HA^-), **7** (HA^-) and **9** (HA^- and A^{2-}), whereas the inclusion reactions of **2** (HA^-), **6** (HA^-) and **8** (HA^-) were found to proceed as one-step processes. The shape and size of the alkyl substituents, R^3 and R^5, and the charge of the phenol moiety are crucial steric, electronic and solvation factors that determine the reaction mechanism.

Directional binding

It should be emphasized that the determination of the direction for inclusion is important in order to clarify the reaction mechanism. When this is established, the relationship between the rate and mechanism for the inclusion reaction of α-CD_x can be considered. From CPK molecular model considerations, both the 2,6-dimethylphenol moiety in **7** and **9**, the 2-*tert*-butylphenol moiety in **6**, and the 2,6-diisopropylphenol moiety in **8** are too large to be included into the α-CD_x cavity. It is therefore clear that the naphthalene-2-sulfonate moiety of **6**, **7**, **8** and **9** is the first incorporated group into the α-CD_x cavity. Thus the rate-controlling step in the first process may be desolvation at the periphery of $-SO_3^-$ group when the guest is included and released from the cavity. The representative rate constants k_{+1} for the desolvation step in **7** (HA^-) and **9** (HA^- and A^{2-}) with α-CD_x were found to be in the order of *ca.* 5×10^3–10^4 dm^3 mol^{-1} s^{-1}.

In the case of **2**, **3** and **4**, the assignment of the direction is more complicated because both directions (A and B) may be possible. By comparison of steric and charge factors of the inclusion reactions of **11** (HA^- and A^{2-}) and **2** (HA^- and A^{2-}), an unambiguous assignment for direction may be possible as shown in Scheme 1 (various arrows denote the inclusion or release processes of α-CD_x).

Compared with **11** (HA^-), the rate constants for inclusion and release of **11** (A^{2-}) is very small, which supports the assignment of direction A.[2,3c] In these systems, inclusion from

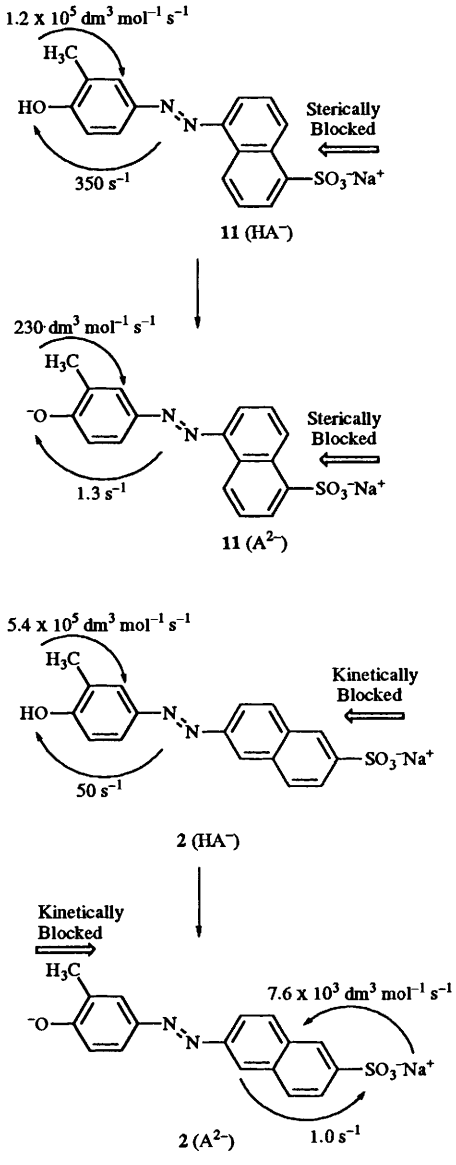

Scheme 1

Table 2 Rate and equilibrium constants[a] for the inclusion reactions of α-cyclodextrin with some 2-naphthylazophenol guests

Guest molecule	k_{+1}/dm^3 mol^{-1} s^{-1}	k_{-1}/s^{-1}	K_1/dm^3 mol^{-1}	k_{+2}/s^{-1}	k_2/s^{-1}	$K_f(K_f')$/dm^3 mol^{-1}
2 (HA^-) R^3 = Me	5.4×10^5	50	10 800	*b*	*b*	11 000
2 (A^{2-})	7.6×10^3	~1[c]	~7 600	*d*	~0.1	9 700
3 (HA^-) R^3 = Et	2.2×10^4	3.0	7 300	*d*	~0.8	14 000
3 (A^{2-})	5.0×10^3	2.9	1 700	0.21	0.1	6 900
4 (HA^-) R^3 = Pr	2.0×10^4	5.5	3 600	*d*	*d*	9 800
6 (HA^-) R^3 = Bu^t	3.1×10^2	0.57	540	*b*	*b*	1 300
7 (HA^-) R^3,R^5 = Me	5.4×10^3	4.0	1 400	>0.3	~0.3	5 000
8 (HA^-) R^3,R^5 = Pr^i	5.7×10^2	1.3	440	*b*	*b*	1 200
9 (HA^-) R^3,R^5 = Me	1.2×10^4	9.0	1 400	0.45	0.2	5 800
9 (A^{2-})	9.0×10^3	12	750	0.88	0.15	5 400

[a] At 25 °C and I = 0.1 mol dm^{-3} (NaCl). [b] No signal. [c] The intercept (k_{-1}) is too small. [d] The value of $k_{slow} - k_{-2}$ is too small.

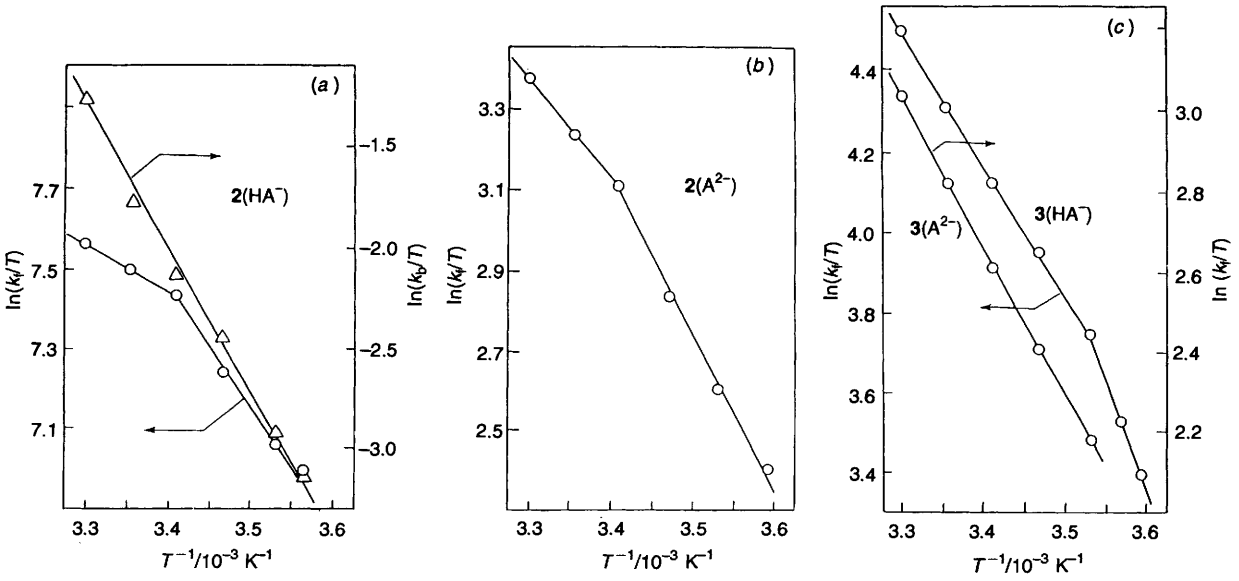

Fig. 1 Eyring plots showing the temperature dependence of the forward and backward rate constants (k_f and k_b) for the inclusion reactions of α-cyclodextrin: (*a*) plots of $\ln(k_f/T)$ and $\ln(k_b/T)$ *versus* T^{-1} for the **2** (HA^-)/α-CD_x system; (*b*) plot of $\ln(k_f/T)$ *versus* T^{-1} for the **2** (A^{2-})/α-CD_x system; (*c*) plots of $\ln(k_f/T)$ for **3** (HA^-)/α-CD_x and $\ln(k_f/T)$ for **3** (A^{2-})/α-CD_x *versus* T^{-1}. Enthalpic and entropic components ($\Delta H‡$ and $\Delta S‡$) were obtained from the slope and the intercept, respectively.

Table 3 Activation parameters for the fast step of the inclusion reactions of **2** and **3** with α-cyclodextrin at 25 °C[a]

Guest molecule	$\Delta G_f^‡$	$\Delta H_f^‡$(HT)	$\Delta S_f^‡$(HT)	$\Delta H_f^‡$(LT)	$\Delta S_f^‡$(LT)
2 (HA^-)[b]	40.3	9.96	−101	26.6	−46.0
2 (A^{2-})	50.9	20.0	−103	33.5	−58.2
3 (HA^-)	48.2	27.4	−69.8	43.7	−15.1
3 (A^{2-})	51.9	31.0	−70.0	—	—

[a] At I = 0.1 mol dm^{-3} (NaCl). $\Delta G_f^‡$ and $\Delta H_f^‡$ in kJ mol^{-1} and $\Delta S_f^‡$ in J mol^{-1} K^{-1}. [b] The temperature dependence of the backward rate constant k_b is obtained in this system. The values of activation parameters, $\Delta G_b^‡$, $\Delta H_b^‡$ and $\Delta S_b^‡$ are evaluated to be 63.3 kJ mol^{-1}, 60.5 kJ mol^{-1} and −9.4 J mol^{-1} K^{-1}, respectively.

direction B (naphthalene-1-sulfonate moiety) is sterically blocked. On the other hand, the determination of the direction of inclusion of **2** (HA^- and A^{2-}) is more interesting. Judging from the similar rate data between **11** (HA^-) and **2** (HA^-) shown in Scheme 1, the preferred site for inclusion of **2** (HA^-) is the 2-methylphenol moiety (direction A). However, inclusion of the deprotonated species A^{2-} from direction A is largely suppressed as observed in **11** (A^{2-}); hence **2** (A^{2-}) undergoes preferential inclusion from direction B. Since inclusion of **2** (A^{2-}) from direction A is potentially allowed, this type of blocking due to the $-O^-$ charge is thought to be *kinetic* rather than steric.

Activation parameters

The activation parameters are determined from the temperature dependence (278–303 K) of the forward and backward rate constants (k_f and k_b). The rate constants k_f and k_b correspond to those (k_{+1} and k_{-1}) for the fast step in eqn. (6). The temperature dependence of the rate constant k_f (k_b) is given by eqn. (9), which can be rewritten in the form of eqn. (10), where

$$k_f = (kT/h) \exp(-\Delta G_f^‡/RT) \quad (9)$$

$$\ln(k_f/T) = \ln(k/h) - (\Delta H_f^‡/RT) + \Delta S_f^‡/R \quad (10)$$

k, R and h are the Boltzmann, gas and Planck constants, respectively. Some plots of $\ln(k_f/T)$ and $\ln(k_b/T)$ *versus* $1/T$ are shown in Fig. 1. The activation free energy ($\Delta G_f^‡$), enthalpic ($\Delta H_f^‡$) and entropic ($\Delta S_f^‡$) components are given in Table 3.

The sharp inflections already reported[3c] are also observed in the plots of $\ln k_f$ *vs.* T^{-1} of the **2** (HA^- and A^{2-}) and **3** (HA^-) guest systems. These inflections in the Eyring plot may be regarded as indicative of the structural change of the reactants and/or the change in the rate-determining step of the reaction in the lower temperature range.[3c]

Since the entropy of freezing of the translational or rotational freedoms of the guest molecule would dominate the overall $\Delta S_f^‡$ in the associative interchange mechanism,[3c] an entropy term is expected to be negative and unfavourable to the Gibbs energy term. In our case, the $\Delta S_f^‡$ has a negative value and its contribution ($-T\Delta S_f^‡$) to the Gibbs energy term ($\Delta G_f^‡$) is estimated to be *ca.* 40–70%. In the backward step, the contribution of $\Delta S_b^‡$ to the Gibbs term $\Delta G_b^‡$ is very small.[3c,d] The activation enthalpy becomes larger in the lower temperature range [$\Delta H_f^‡$(HT) ⟶ $\Delta H_f^‡$(LT)] and is reasonably compensated by the entropy terms [$\Delta S_f^‡$(HT) ⟶ $\Delta S_f^‡$(LT)]. Plots of $\Delta H_f^‡$ *versus* $\Delta S_f^‡$ show a good linear relationship (Fig. 2).

The isokinetic relationship [$\Delta H_f^‡ = 270(26)\ \Delta S_f^‡ + 4.8 \times 10^4$ (1.8×10^3), where the values in parentheses denote the standard deviation] in Fig. 2 does not seem to be dependent on substituents as reported previously.[3c] Interestingly, the isokinetic temperature[6] β = 270 K is close to the freezing point of solvent water to within experimental error. Estimated differences in the activation parameters such as $\Delta\Delta H_f^‡$[= $\Delta H_f^‡$(HT) − $\Delta H_f^‡$(LT) = *ca.* 14–17 kJ mol^{-1}] and $\Delta\Delta S_f^‡$[= $\Delta S_f^‡$(HT) − $\Delta S_f^‡$(LT) = *ca.* 45–55 J mol^{-1} K^{-1}] are nearly constant irrespective of the reaction systems for **2** (HA^- and A^{2-}) and **3** (A^{2-}), which suggests that the inflections in the Eyring plot are indicative of similar phenomena.

^{1}H NMR spectroscopy

The azo guest molecule **4** has distinctive and readily interpretable NMR spectra. α-CD_x seems to bind strongly with **4** for which its cavity is compatible. Interestingly, in the β-CD_x system, only one inclusion complex is formed, but in the α-CD_x system, two and/or three states of the inclusion complex are observed. Thus, the ^{1}H NMR spectra of the α-CD_x inclusion complexes of **4** demonstrate more complicated signals than the corresponding β-CD_x inclusion complexes because of the existence of intermediates in the equilibrated solution [eqn. (6)]. Representative examples of the ^{1}H NMR spectra of **4** (HA^-) and its complex are shown in Fig. 3(*a*) and 3(*b*), respectively, and the following points are noted.

(1) The signals of the methyl, methylene (α), and methylene (β) protons in the propylphenol moiety of **4** (HA^-) are shifted downfield as the increments of α-CD_x were added ($\Delta\delta$ = 0.36–0.42, 0.76–0.83 and 052–0.57 ppm, respectively, as depicted in Fig. 3A). These protons were chosen because their chemical shifts are most sensitive to complexation, although similar but less distinguishable signal changes were also observed with other protons (Fig. 3B).

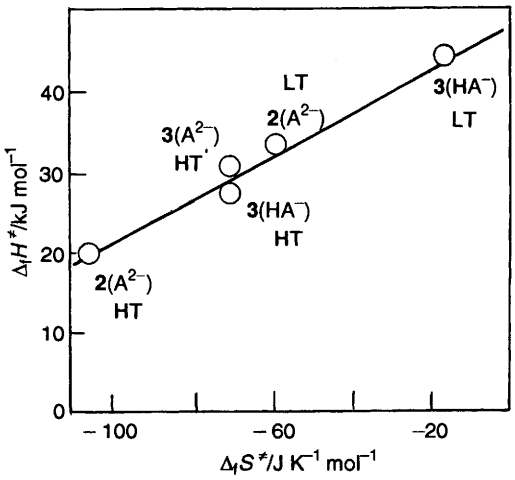

Fig. 2 Isokinetic plot of $\Delta H^{\ddagger}$ *versus* $\Delta S^{\ddagger}$. The slope yields an isokinetic temperature of 270 K. Data for **2** (A^{2-}), **3** (HA^-) and **3** (A^{2-}) guest molecules were taken from Table 3. HT and LT denote the higher temperature and lower temperature regions in the plot of Fig. 1.

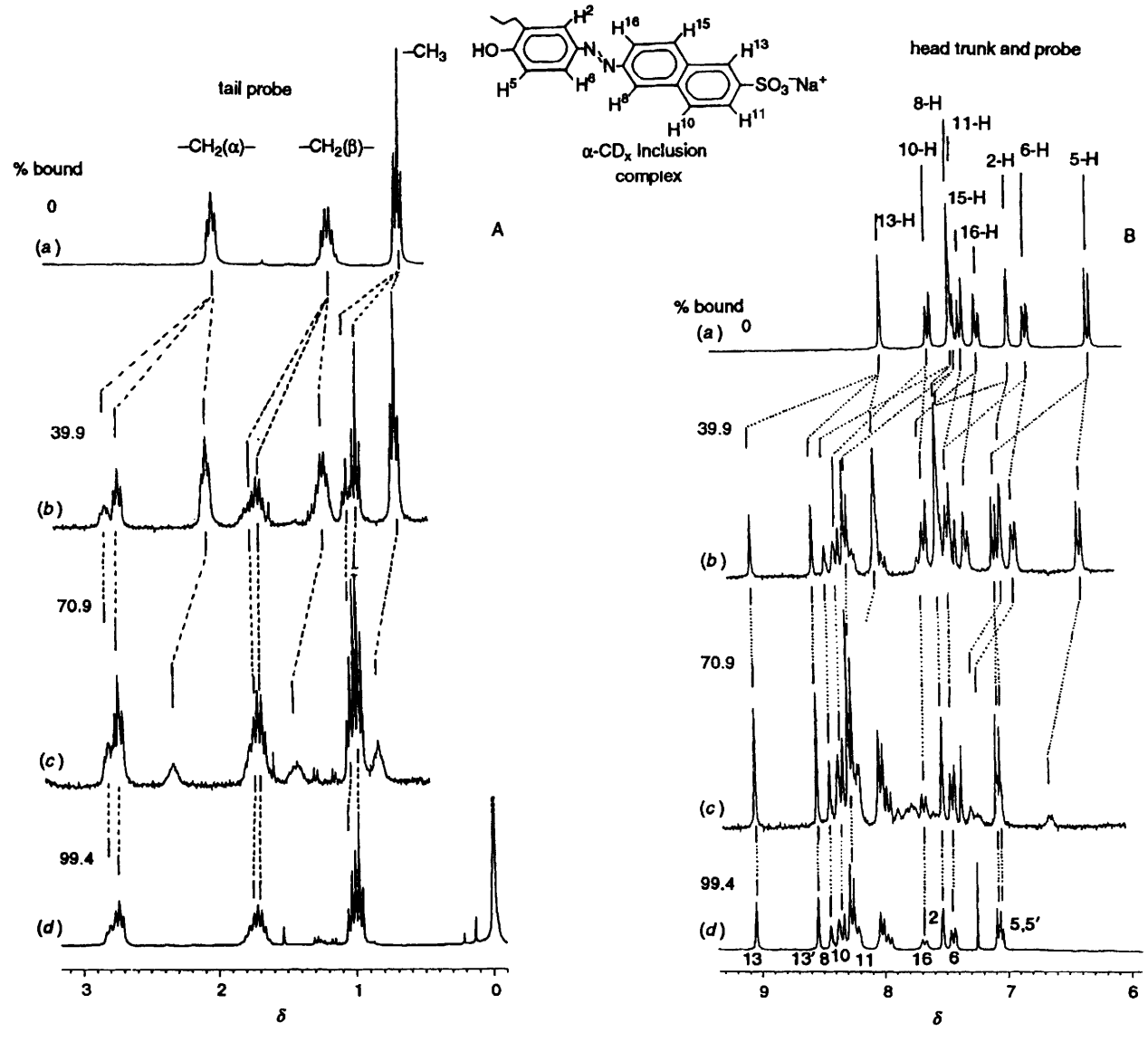

Fig. 3 ^{1}H NMR spectra of the α-cyclodextrin complex of **4** (HA^-) in D_2O at 25 °C. The guest concentration is *ca.* 0.0327–0.0358 mol dm^{-3}: A, resonances of the propylphenol moiety of **4** (HA^-): (*a*) guest **4** (HA^-) only; (*b*)–(*d*) **4** (HA^-) and 0.40, 0.72 and 1.45 equiv. of α-cyclodextrin, respectively; B, resonances of the sulfonaphthalene moiety of **4** (HA^-): (*a*) guest **4** (HA^-) only; (*b*)–(*d*) **4** (HA^-) and 0.40, 0.72 and 1.45 equiv. of α-cyclodextrin, respectively.

Table 4 ^{1}H NMR (270 MHz) data for the α-cyclodextrin inclusion complexes of the acid form (HA^-) of sodium 2-(3-propyl-4-hydroxyphenylazo)naphthalene-6-sulfonate, **4** (HA^-)

	CH_3[b]			$CH_2(\beta)$			$CH_2(\alpha)$			H^5		
Bound(%)[a]	δ_a	δ_b	δ_c	δ_a	δ_b	δ_c	δ_a	δ_b	δ_c	δ_a	δ_b	δ_c
0	0.61 (δ_{free})			1.13 (δ_{free})			1.97 (δ_{free})			6.2 (δ_{free})		
3.2	0.63 (94)[d]	0.95 (3.9)	c (2)	1.14 (96)	c	c (4)	1.98 (96)	2.68	c (4)	6.27	c	c
10.6	0.63 (82)	0.95 (12)	1.03 (6)	1.15 (84)	1.65	1.67 (16)	2.00 (84)	2.68	2.80 (16)	6.29	c	c
20.3	0.65 (76)	0.95 (15)	1.03 (9)	1.17 (73)	1.65	1.67 (27)	2.01 (73)	2.69 (17)	2.79 (10)	6.31	e	e
28.9	0.66 (64)	0.95 (24)	1.03 (12)	1.18 (65)	1.65	1.67 (35)	2.03 (66)	2.69 (23)	2.79 (11)	6.33	e	e
39.9	0.68 (53)	0.96 (31)	1.03 (16)	1.21 (55)	1.65	1.67 (45)	2.06 (56)	2.71 (30)	2.81 (14)	6.37	e	e
58.4	0.74 (32)	0.97	1.03 (68)	1.30 (34)	1.65	1.67 (66)	2.16 (32)	2.72 (47)	2.80 (22)	6.47	e	e
70.9	0.83 (18)	0.97	1.03 (82)	1.42 (18)	1.65	1.67 (82)	2.33 (17)	2.73 (58)	2.80 (30)	6.69 (18)	7.06	7.08 (82)
87.9	f	0.97	1.03 (100)	f	1.65	1.67 (100)	f	2.73 (~65)	2.80 (~35)	f	7.06	7.08 (100)
94.9	f	0.97	1.03 (100)	f	1.65	1.67 (100)	f	2.73 (~64)	2.80 (~36)	f	7.06	7.08 (100)
99.4	f	0.97	1.03 (100)	f	1.65	1.67 (100)	f	2.73 (~65)	2.80 (~35)	f	7.06	7.08 (100)

[a] Bound(%) is calculated using the value (9.8×10^3 dm^3 mol^{-1}) of the formation constant, K_f (=[complex]/[guest]·[α-CD_x]). [b] Each $\delta_{a,b,c}$ is the chemical shift of the tail or head protons (ppm) in three environments relative to external TMS (1% in $CDCl_3$) in D_2O. Estimated error is within ± 0.02 ppm. [c] The signal is too small to detect. The percentage is smaller than 1%. [d] Parentheses denote the relative ratio of the bound guest molecule in the three states (a), (b) and (c). These ratios can be evaluated from the integral curve of each proton. [e] Two signals are overlapped. [f] Not detectable.

Table 5 ^{1}H NMR (270 MHz) data for the α-cyclodextrin inclusion complexes of the base form (A^{2-}) of sodium 2-(3-propyl-4-hydroxyphenylazo)naphthalene-6-sulfonate, **4** (A^{2-})

	CH_3[a]		$CH_2(\beta)$[a]		$CH_2(\alpha)$[a]		H^5	
Bound(%)	δ_{free}	δ_c	δ_{free}	δ_c	δ_{free}	δ_c	δ_{free}	δ_c
0	0.94 (100)		1.56 (100)		2.49 (100)		6.64 (100)	
4.0	0.94 (< 100)	b	1.56 (< 100)	b	2.50 (< 100)	b	6.64 (< 100)	b
12.1	0.94 (85.5)	1.00 (14.5)	1.56	b	2.50 (85.4)	2.63 (14.6)	6.64	b
19.5	0.94	1.00	1.57	1.63	2.50 (70.9)	2.63 (28.8)	6.65	6.68
31.2	0.94	1.00	1.57	1.63	2.51 (64)	2.62 (36)	6.65	6.68
69.5	0.94	1.00	1.59	1.65	2.53 (38)	2.62 (62)	6.65	6.68
95.1		1.00	b	1.65	b	2.62	b	6.68
99.1		1.00		1.64		2.61		6.67

[a] The value of $\delta_c - \delta_{free}$ is 0.06, 0.08, 0.13 and 0.03 for the CH_3, $CH_2(\beta)$, $CH_2(\alpha)$, and H^5 protons, respectively. [b] The signal is too small to detect.

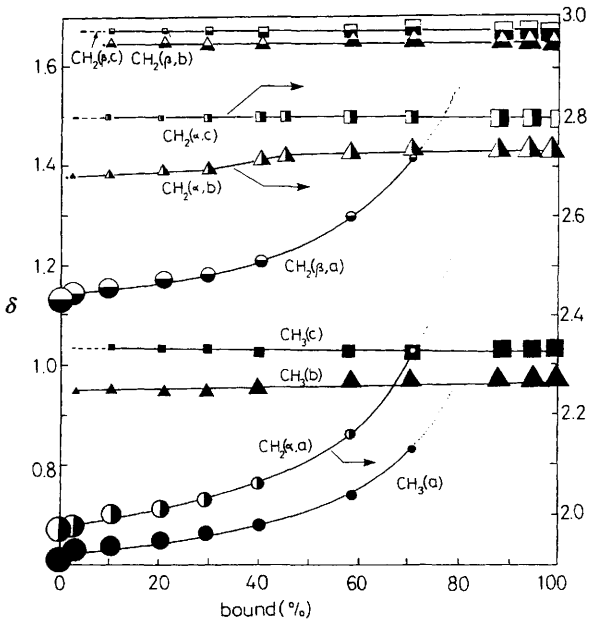

Fig. 4 Plots of the observed chemical shifts (δ) of the protons of CH_3–, $-CH_2(\alpha)-$ and $-CH_2(\beta)-$ in the propylphenol moiety of **4** (HA^-) upon titration with α-cyclodextrin. The bound(%) denotes the % ratio ([bound guest]/[total guest]) × 100.

(2) Three types of signal reflecting the different environments of the protons within the α-CD_x cavity were observed for CH_3–, $-CH_2(\alpha)-$ and $-CH_2(\beta)-$ protons. An unusual shift in the proton signal [type (a)] was observed as shown in Fig. 4 and Table 4 (δ_a). This signal moves gradually downfield at lower bound(%) and abruptly shifts downfield at *ca.* 60 bound(%) as shown in Fig. 4. The ratio of this signal to the other types of signal decreases with increasing the bound(%) as depicted in Table 4. The type (*a*) signal has not so far been found for the simple inclusion reaction (G + α-$CD_x \rightleftharpoons$ G-αCD_x). Interestingly, this signal disappears completely at bound(%) = 100.

(3) As shown in Fig. 4, the chemical shifts of the other two sets of signals [types (b) and (c)] appear at a constant position irrespective of the bound(%), indicating the slower exchange process compared with the NMR timescale. Their chemical shifts (δ_b and δ_c) were closely situated in close proximity (Fig. 4).

These complicated splitting patterns observed in the **4** (HA^-)/α-CD_x system disappeared in the **4** (A^{2-})/α-CD_x and **4** (HA^- and A^{2-})/β-CD_x systems as shown in Fig. 5A and 5B. In these systems, no intermediates were detected.

Generally, the ^{1}H NMR spectra of the guest/cyclodextrin system consist of only one set of concentration-dependent resonances, indicating that only one type of inclusion occurs and that chemical exchange of the type of G + $CD_x \rightleftharpoons$ G–CD_x is rapid compared with the NMR timescale. The observed chemical shift (δ_{obsd}) for the fast exchange inclusion equilibrium can be given by eqn. (9), where δ_G, $\delta_{G\text{-}CD_x}$, and

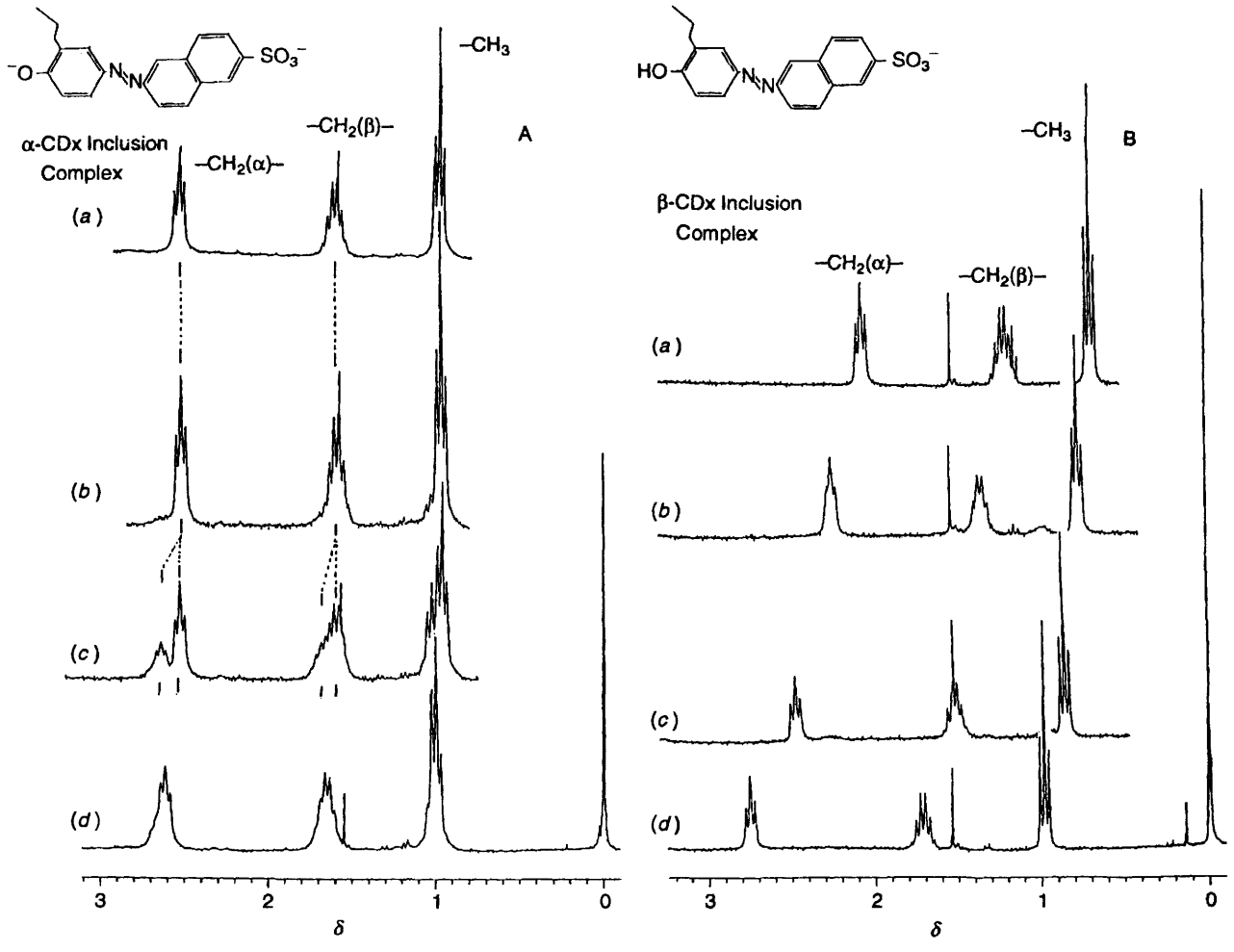

Fig. 5 ^{1}H NMR spectra of the α-cyclodextrin complex of **4** (A^{2-}) and β-cyclodextrin complex of **4** (HA^-) in D_2O at 25 °C. The guest concentration is *ca.* 0.0324 mol dm^{-3} for the α-CD_x and 0.0127 mol dm^{-3} for the β-CD_x system, respectively: A, resonances of the propylphenol moiety of **4** (A^{2-}): (*a*) guest **4** (A^{2-}) only; (*b*)–(*d*) **4** (A^{2-}) and 0.124 [Bound(%) = 12.1], 0.320 (31.2), and 1.65 (99.0) equiv. of α-cyclodextrin, respectively; B, resonances of the propylphenol moiety of **4** (HA^-): (*a*) guest **4** (HA^-) only; (*b*)–(*d*) **4** (HA^-) and 0.23 (22.9), 0.48 (47.1) and 1.52 (98.2) equiv. of β-cyclodextrin, respectively.

$$\delta_{obsd} = \frac{[G]}{[G]_T}\delta_G + \frac{[G\text{–}CD_x]}{[G]_T}\delta_{G\text{–}CD_x} \quad (9)$$

$[G]_T$ denote the chemical shifts of G and G–CD_x, and the total concentration of the guest.[7,8] On addition of cyclodextrin, the proton resonances of the guest underwent a remarkable downfield shift and should approach a saturated value in the higher CD_x concentration range. This is the case for a system such as **4** (HA^-)/β-CD_x in which only fast one-step inclusion is observed (Fig. 5B). The **4** (HA^-)/α-CD_x system does not participate in the simple exchange process G + $CD_x \rightleftharpoons$ G–CD_x. Therefore, the data in Table 4 were not used as an independent method of determining the K_f values in the usual way by a curve-fitting procedure, as is commonly done in host–guest chemistry.

The above-mentioned ^1H NMR and rate data for the **4** (HA^-)/α-CD_x system may be simply interpreted as the dynamic behaviour of the guest illustrated in Scheme 2 and result from the exchange of the guest between three different environments, (a), (b) and (c). This exchange process may be regarded as a two-site directional inclusion into the α-CD_x cavity. In the two-site directional inclusion mechanism, the H^5, $CH_3CH_2CH_2$– and H^{13} protons of **4** (HA^-) are useful probes which provide the insight to the structure of the intermediate and/or the final inclusion complex (Scheme 2). It is assumed in Scheme 2 that

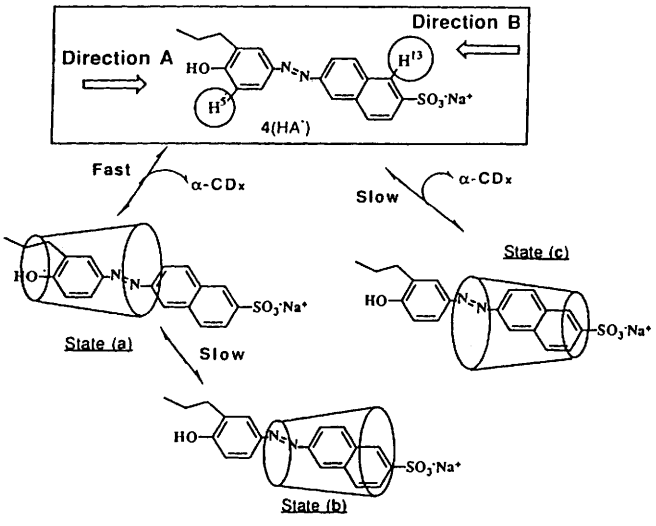

Scheme 2

there are fast [state (a)] and slow [states (b) and (c)] exchange processes between free and bound guest **4** (HA^-) with α-CD_x. The guest **4** (HA^-) in state (a) would be more slowly converted into the deeply bound guest in state (b). There is a considerable difference between δ_a and δ_b (δ_c). However, such a large difference is not observed between δ_b and δ_c (Table 4). Therefore, the difference in the two environments (b) and (c) is quite small. The difference between this two-site directional mechanism (Scheme 2) and the kinetic mechanism as shown in eqn. (6) was not detected in principle by the optical stopped-flow method.

Finally, in the case of the ^1H NMR spectra of the **4** (A^{2-})/α-CD_x system, the peaks for the bound guest in states (a) and (b) were not observed [Fig. 5(*a*) and Table 5]. This is because of the kinetically controlled effect whereby inclusion from direction A is blocked owing to the negative charge of the $-O^-$ group (see Scheme 1). Therefore, only the peak for state (c) is observed in the **4** (A^{2-})/α-CD_x system. Furthermore, in the guest system **8** (HA^-) where inclusion from direction A is fully blocked owing to steric hindrance from the 3,5-diisopropyl groups, the bound guest in state (a) is not detected in its ^1H NMR spectrum.

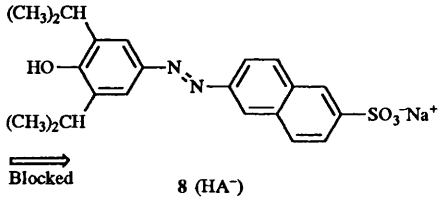

8 (HA^-)

References

1 D. W. Griffith and M. L. Bender, *Adv. Catal.*, 1973, **23**, 209; J. Emert and R. Breslow, *J. Am. Chem. Soc.*, 1975, **97**, 670; I. Tabushi, K. Shimokawa, H. Shirakata and K. Fujita, *J. Am. Chem. Soc.*, 1976, **98**, 7855; R. Breslow, *Acc. Chem. Res.*, 1980, **13**, 170; R. Breslow, M. F. Czarniecki, J. Emert and H. Hamaguchi, *J. Am. Chem. Soc.*, 1980, **102**, 762; I. Tabushi, *Acc. Chem. Res.*, 1982, **15**, 66; C. Sirlin, *Bull. Soc. Chim. Fr.*, 1984, 5; O. S. Tee and J. J. Hoeven, *J. Am. Chem. Soc.*, 1989, **111**, 8318; R. Breslow, *Acc. Chem. Res.*, 1991, **24**, 317; R. Breslow and B. Zhang, *J. Am. Chem. Soc.*, 1994, **116**, 7893; R. Corradini, A. Dossena, G. Impelizzeri, G. Maccarrone, R. Marchelli, E. Rizzarelli, G. Sartor and G. Vecchio, *J. Am. Chem. Soc.*, 1994, **116**, 10 267; T. J. Wenzel, M. S. Bogyo and E. L. Lebeau, *J. Am. Chem. Soc.*, 1994, **116**, 4858; A. V. Eliseev and H.-J. Schneider, *J. Am. Chem. Soc.*, 1994, **116**, 6081.

2 F. Cramer, W. Saenger and H.-Ch. Spatz, *J. Am. Chem. Soc.*, 1967, **89**, 14.

3 (*a*) N. Yoshida and M. Fujimoto, *Chem. Lett.*, 1980, 231 and 1377; (*b*) N. Yoshida and M. Fujimoto, *J. Chem. Res.*, 1985, 1013; (*c*) N. Yoshida and M. Fujimoto, *J. Phys. Chem.*, 1987, **91**, 6691; (*d*) N. Yoshida, A. Seiyama and M. Fujimoto, *J. Phys. Chem.*, 1990, **94**, 4246; (*e*) N. Yoshida and K. Hayashi, *J. Chem. Soc., Perkin Trans. 2.*, 1994, 1285; (*f*) N. Yoshida and Y. Fujita, *J. Phys. Chem.*, 1995, **99**, 3671.

4 (*a*) R. P. Rohrbach and J. F. Wojcik, *Carbohydr. Res.*, 1981, **92**, 177; (*b*) A. Örstan and J. F. Wojcik, *Carbohydr. Res.*, 1985, **143**, 43; (*c*) A. Örstan and J. F. Wojcik, *Carbohydr. Res.*, 1988, **176**, 149.

5 A. Hersey and B. H. Robinson, *J. Chem. Soc., Faraday Trans. 1*, 1984, **80**, 2039.

6 N. S. Isaacs, *Physical Organic Chemistry*, Longman: New York, 1987, p. 102; S. M. Lui, W. Liang, A. Soriano and J. A. Cowan, *J. Am. Chem. Soc.*, 1994, **116**, 4531.

7 N. Yoshida, A. Seiyama and M. Fujimoto, *J. Phys. Chem.*, 1990, **94**, 4254.

8 R. J. Bergeron, M. A. Channing, G. J. Gibeily and D. M. Pillor, *J. Am. Chem. Soc.*, 1977, **99**, 5146.

Paper 5/03807C
Received 13*th June* 1995
Accepted 21*st July* 1995